*Magnetochemistry* **2015**, *1*, 72-82; doi:10.3390/magnetochemistry1010072

OPEN ACCESS

*magnetochemistry*

**ISSN 2312-7481**

www.mdpi.com/journal/magnetochemistry

*Article*

# Abrupt Spin Transition and Chiral Hydrogen-Bonded One-Dimensional Structure of Iron(III) Complex $[Fe^{III}(Him)_2(hapen)]SbF_6$ (Him = imidazole, $H_2$hapen = *N,N′*-bis(2-hydroxyacetophenylidene)ethylenediamine)

**Takahiro Ueno [1], Kyohei Miyano [1], Daisuke Hamada [1], Hiromasa Ono [1], Takeshi Fujinami [1], Naohide Matsumoto [1,*] and Yukinari Sunatsuki [2]**

[1] Department of Chemistry, Faculty of Science, Kumamoto University, Kurokami 2-39-1, Chuo-ku, Kumamoto 860-8555, Japan; E-Mails: 153d8024@st.kumamoto-u.ac.jp (T.U.); 159d8049@st.kumamoto-u.ac.jp (K.M.); 147d8026@st.kumamoto-u.ac.jp (D.H.); 148d8017@st.kumamoto-u.ac.jp (H.O.); namipon0319@gmail.com (T.F.)

[2] Department of Chemistry, Faculty of Science, Okayama University, Tsuchima-naka, Okayama 700-0082, Japan; E-Mail: sunatuki@okayama-u.ac.jp

* Author to whom correspondence should be addressed; E-Mail: naohide@aster.sci.kumamoto-u.ac.jp; Tel./Fax: +81-96-342-3390.

Academic Editor: Guillem Aromí

*Received: 2 October 2015 / Accepted: 9 November 2015 / Published: 11 December 2015*

---

**Abstract:** Solvent-free spin crossover (SCO) iron(III) complex, $[Fe^{III}(Him)_2(hapen)]SbF_6$ (Him = imidazole, $H_2$hapen = *N,N′*-bis(2-hydroxyacetophenylidene)ethylenediamine), is synthesized. The $Fe^{III}$ ion has an octahedral coordination geometry, with $N_2O_2$ donor atoms of hapen and $N_2$ atoms of two imidazoles at the axial positions. The saturated five-membered chelate ring of hapen moiety assumes a gauche-type δ- or λ-conformation to give chiral species of δ-$[Fe^{III}(Him)_2(hapen)]^+$ or λ-$[Fe^{III}(Him)_2(hapen)]^+$. One imidazole is hydrogen-bonded to phenoxo oxygen atom of hapen of the adjacent unit to give a hydrogen-bonded chiral one-dimensional structure, $\{\delta\text{-}[Fe^{III}(Him)_2(hapen)]^+\}_{1\infty}$ or $\{\lambda\text{-}[Fe^{III}(Him)_2(hapen)]^+\}_{1\infty}$. The adjacent chains with the opposite chiralities are arrayed alternately. The temperature dependences of the magnetic susceptibilities revealed an abrupt one-step spin transition between high-spin ($S$ = 5/2) and low-spin ($S$ = 1/2) states at the spin transition temperature of $T_{1/2}$ = 105 K. The crystal structures were determined at 296 and 100 K, where the populations of HS:LS of high- and low-spin ratio are evaluated to be 1:0 and 0.3:0.7, respectively, based on magnetic measurements. During the spin transition from 296 K to

100 K, the average Fe–N distance and O–Fe–O angle decrease to a regular octahedron by 0.16 Å and 13.4°, respectively. The structural change in the coordination environment is transmitted to the adjacent spin crossover (SCO) sites along the chiral 1D chain through hydrogen-bonds. The abrupt SCO profile and the spin transition temperature for the isomorphous compounds $[Fe^{III}(Him)_2(hapen)]Y$ ($Y = PF_6$, $AsF_6$, $SbF_6$) are ascribed to the chiral hydrogen-bonded 1D structure and chain-anion interaction.

**Keywords:** iron(III) complex; imidazole; $N_2O_2$ Schiff-base; hydrogen-bond; one-dimensional structure; chiral chain

## 1. Introduction

Spin crossover (SCO) is a representative phenomenon of molecular bistability and an inter-conversion between high-spin (HS) and low-spin (LS) states can occur by external physical perturbations [1]. While SCO originates from single molecule, steepness, multi-step, and hysteresis in a SCO profile are brought from the cooperative effect operating between the SCO sites [1]. Among the interactions leading to a cooperative effect, it is well known that the hydrogen bond plays a crucial and effective role [2].

We have focused on SCO molecules exhibiting intermolecular hydrogen bonds [3,4] and investigated how the hydrogen bond affects the SCO properties. One of the molecular systems is an $Fe^{III}$ complex with a salen-type $N_2O_2$ ligand and imidazole $[Fe^{III}(Him)_2(salen\text{-}type)]^+$ (Scheme 1). Nishida [5,6] reported the first such SCO $Fe^{III}$ complex as a simple model compound of the Fe sites in some heme proteins. Later, Matsumoto [7–9], Murray [10,11], and Real [12] reported the analogous $Fe^{III}$ complexes, and their works revealed the relevant structural factors to determine the SCO properties of these types of complexes [13].

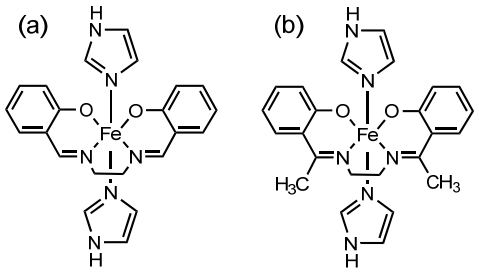


**Scheme 1.** Structures of $[Fe^{III}(Him)_2(salen)]^+$ (**a**) and $[Fe^{III}(Him)_2(hapen)]^+$ (**b**).

Previously, we reported an abrupt SCO $Fe^{III}$ complex $[Fe^{III}(Him)_2(hapen)]PF_6$ [14] and a hysteresis SCO $Fe^{III}$ complex $[Fe^{III}(Him)_2(hapen)]AsF_6$ [15], where SCO $Fe^{III}$ compounds, in general, exhibit gradual spin equilibrium and show no thermal hysteresis [1]. The unusual SCO property of the SCO $Fe^{III}$ complex is due to the molecular distortion of the complex-cation $[Fe^{III}(Him)_2(hapen)]^+$ and the chiral one-dimensional structure constructed by the inter-cation O···HN hydrogen bond between a phenoxo oxygen and an imidazole nitrogen. Unfortunately, only the structure in the high-spin HS state is determined for the $PF_6$ and $AsF_6$ salts. In this study, we have synthesized $SbF_6$ salt in which the spin transition temperature shifted to a higher temperature. We could determine the structures at the HS and

LS states and know the molecular distortion of the complex-cation during the spin transition. Further, we could consider the abrupt SCO profile and the shift of the spin transition temperature within the frame work of a 1D structure.

## 2. Results and Discussion

### *2.1. Synthesis and Characterization*

The $[Fe^{III}(Him)_2(hapen)]SbF_6$ complex was prepared by the method adopted for the $PF_6$ and $AsF_6$ salts [14,15]. The mixed solution of precursor $Fe^{III}$ complex $[Fe^{III}Cl(hapen)]\cdot 0.5CH_3OH$, imidazole, and $NaSbF_6$, in a 1:10:1 molar ratio in methanol, precipitates black plate-like crystals. The $SbF_6$ salt exhibits a thermochromism, both in the solution and solid states. The red color of the dilute ethanol solution at ambient temperature changes to green at the temperature of liquid nitrogen, where red and green are typical colors for the HS and LS $Fe^{III}$ complexes with the Schiff-base ligands with $N_4O_2$ donor atoms [16]. In the solid state, the black color of the ground sample at room temperature changes to green at the temperature of liquid-nitrogen. The thermochromism demonstrates that the complex is a SCO complex, both in the solid and solution states.

### *2.2. Magnetic Properties*

The molar magnetic susceptibilities ($\chi_M$) of the polycrystalline sample were measured in the temperature range of 5–300 K, under an applied magnetic field of 0.5 T at a sweep rate of 0.5 K $min^{-1}$. The magnetic susceptibility was measured by lowering the temperature from 300 to 5 K as the first run, and, subsequently, by elevating the temperature from 5 to 300 K as the second run. The plots of $\chi_M T$ *vs.* $T$ for the present $SbF_6$ salt (blue), together with those of the $PF_6$ (red) and $AsF_6$ (green) salts were measured at the same scan rate and as reported previously [14,15], are shown in Figure 1. Three compounds show a similar, complete abrupt spin transition between the HS ($S$ = 5/2) and LS ($S$ =1/2) states, though $Fe^{III}$ SCO compounds generally exhibit gradual spin equilibrium. The magnetic profile of the $SbF_6$ salt is described briefly. On lowering the temperature from 300 to 5 K, the $\chi_M T$ value keeps the upper plateau value in the temperature region higher than 150 K, decreases abruptly around *ca.* 110 K, and then reaches the lower plateau value in a temperature region lower than 95 K. The spin-transition temperature of the $SbF_6$ salt is evaluated to be $T_{1/2}$ = 105 K.

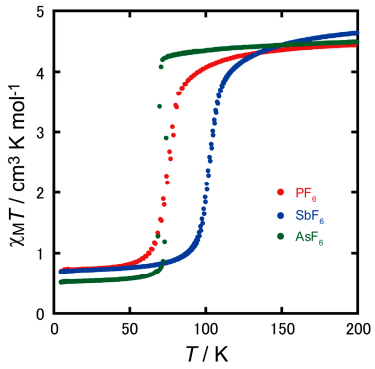


**Figure 1.** $\chi_M T$ *vs.* $T$ plots for $[Fe^{III}(Him)_2(hapen)]SbF_6$ (blue) in the temperature region of 0–200 K, together with those of the $PF_6$ (red) and $AsF_6$ (green) salts.

### *2.3. Crystal Structure of [Fe$^{III}$(Him)$_2$(hapen)]SbF$_6$ at the HS and LS States*

The crystal structures at the HS and LS states were determined at 296 and 100 K. On the basis of the magnetic susceptibility measurements, the populations of HS:LS at 296 and 100 K are evaluated by the equation of $\chi_M(T) = (1 - x)\ \chi_M(HS) + x\chi_M(LS)$, where $\chi_M(HS) = 4.7$ cm$^3$ K mol$^{-1}$ and $\chi_M(LS) = 0.7$ cm$^3$ K mol$^{-1}$ are used as the limiting values, and $\chi_M(100) = 1.9$ cm$^3$ K mol$^{-1}$. The populations of HS:LS at 296 and 100 K were evaluated to be 1:0 and 0.3:0.7, respectively. The structures at 296 and 100 K have an isomorphous structure, demonstrating no phase transition during the spin transition. The crystallographic data are listed in Table 1. Relevant coordination bond distances, angles, and hydrogen-bond distances are given in Table 2.

**Table 1.** Crystallographic Data. of [Fe$^{III}$(Him)$_2$(hapen)]SbF$_6$ at 296 and 100 K.

| **Formula** | **$C_{24}H_{26}N_6O_2FeSbF_6$** | | |
|---|---|---|---|
| formula weight | | 722.10 | |
| crystal system | | monoclinic | |
| space group | | *C2/c* (No.15) | |
| *T*, K | 296 | 100 | Δ, % |
| *a*, Å | 24.915(2) | 24.669(2) | 0.246, 0.98% |
| *b*, Å | 9.6553(7) | 9.2793(6) | 0.376, 3.9% |
| *c*, Å | 25.136(2) | 24.704(2) | 0.432, 1.7% |
| *β*, deg. | 112.256(2) | 109.991(2) | 2.266 |
| *V*, Å$^3$ | 5596.5(7) | 5314.3(6) | 282.2, 5.0% |
| *Z* | 8 | 8 | - |
| $D_{calcd}$, g cm$^{-3}$ | 1.771 | 1.805 | - |
| $\mu$, mm$^{-1}$ | 1.558 | 1.637 | - |
| $R^a$, $Rw^b$ | 0.0992, 0.2712 | 0.0742, 0.1781 | - |

[a] $R = \Sigma||Fo|-|Fc||/\Sigma|Fo|$; [b] $Rw = [\Sigma w(|Fo^2|-|Fc^2|)^2/\Sigma w|Fo^2|^2]^{1/2}$.

The crystallographic unique unit consists of one cation [Fe$^{III}$(Him)$_2$(hapen)]$^+$ and one counter anion SbF$_6^-$. The molecular structure of the [Fe$^{III}$(Him)$_2$(hapen)]$^+$ part at 296 K with the selected atom numbering scheme is shown in Figure 2a,b. The Fe$^{III}$ ion has an octahedral coordination environment with $N_2O_2$ donor atoms of electronically di-negative tetradentate ligand hapen at the equatorial sites, and $N_2$ donor atoms of two imidazoles at the two axial positions. Figure 2b shows the orientations of the two imidazole rings, in which one imidazole ring bisects the angles defined by two N–Fe–O diagonals, and other imidazole ring is oriented near to along the N–Fe–O diagonal. The saturated five-membered chelate ring, involving an ethylenediamine moiety, assumes a gauche conformation, in which C9 and C10 atoms deviate by −0.22 and +0.40 Å from the plane, defined by Fe, N1, and N2 atoms. For the gauche conformation, chiral δ and λ conformations are possible, thus, the complex-cation is either a δ- and λ-[Fe$^{III}$(Him)$_2$(hapen)]$^+$ chiral molecule. The dihedral angle between the $N_2O_2$ coordination plane and the benzene ring (see Figure 2b) is −9.9° and 22.8° for benzene ring A and B, respectively, in which the B ring bound to O2 is quite tilted.

**Table 2.** Bond Distances (Å), Angles (°), and Hydrogen Bond Distances (Å) of $[Fe^{III}(Him)_2(hapen)]SbF_6$ at 296 and 100 K.

| Distance and angle | 296 K | 100 K | Δ (Å, °) |
|---|---|---|---|
| Bond lengths (Å) | | | |
| Fe–N1 | 2.117(10) | 1.935(7) | −0.182 |
| Fe–N2 | 2.116(8) | 1.944(6) | −0.172 |
| Fe–N3 | 2.146(8) | 1.986(6) | −0.160 |
| Fe–N5 | 2.150(9) | 2.005(6) | −0.145 |
| Average <Fe–N> | 2.132 | 1.968 | −0.164 |
| Fe–O1 | 1.882(7) | 1.879(5) | −0.007 |
| Fe–O2 | 1.908(10) | 1.879(6) | −0.029 |
| Average <Fe–O> | 1.895 | 1.879 | −0.016 |
| Bond angles (°) | | | |
| O1–Fe–O2 | 102.5(4) | 89.1(3) | −13.4 |
| O1–Fe–N1 | 88.0(4) | 92.3(3) | +4.3 |
| O2–Fe–N2 | 89.1(4) | 92.6(3) | +3.5 |
| N1–Fe–N2 | 80.5(4) | 86.1(3) | +5.6 |
| N1–Fe–N3 | 88.8(4) | 91.5(3) | +2.7 |
| N1–Fe–N5 | 89.1(4) | 91.0(3) | +1.9 |
| N2–Fe–N3 | 88.9(4) | 89.3(3) | −0.4 |
| N2–Fe–N5 | 85.5(4) | 88.3(3) | +2.8 |
| Hydrogen bond lengths (Å) | | | |
| N6H···O2 * | 2.95(1) | 2.902(8) | - |
| N6H···O1 * | 3.28(2) | 3.03(3) | - |
| F3···N4 | 3.10(3) | 3.104(14) | - |
| F9···N4 | 3.00(2) | 2.891(14) | - |
| F9···N4 * | 3.34(3) | 3.341(18) | - |

* $1/2 - x, 1/2 + y, 1/2 - z$.

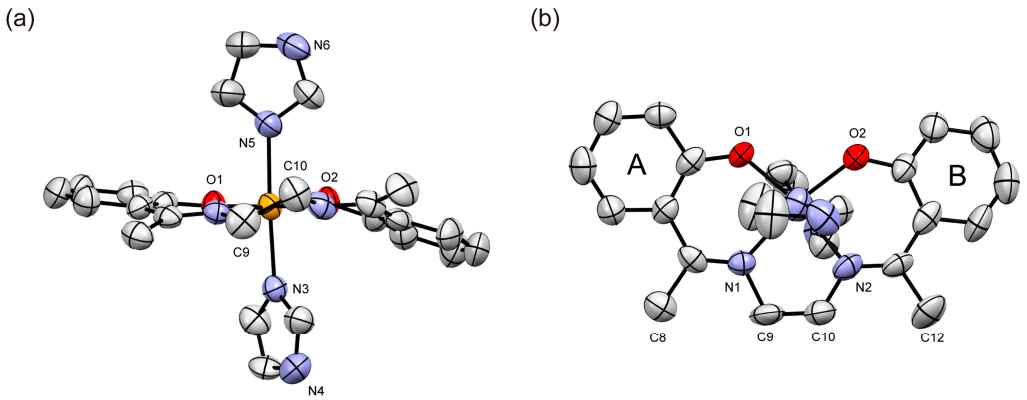


**Figure 2.** (**a**) An ORTEP drawing of λ-$[Fe^{III}(Him)_2(hapen)]^+$ cation of $[Fe^{III}(Him)_2(hapen)]SbF_6$ with the selected atom numbering scheme at 296 K, showing the molecular distortions. The thermal ellipsoids were drawn at the 50% probability level; (**b**) View of the complex-cation projected on hapen, showing the orientations of two imidazole rings.

At 296 K, the four Fe–N bond distances are in the range 2.116(8)–2.150(9) Å, in which the Fe–N (imidazole) distance is slightly longer than the Fe–N (imine) distance. The Fe–O1 distance of 1.882(7) Å is

slightly shorter than the Fe–O2 distance of 1.908(10) Å, where O2 is hydrogen-bonded to N6* of the imidazole group of the adjacent complex-cation and O1 is free from hydrogen bonding. These Fe–N and Fe–O coordination bond distances are consistent with the bond distances reported for HS $Fe^{III}$ complexes with similar Schiff-base ligands [10–15]. The O1–Fe–O2 bond angle of 102.5(4)° is indicative of the HS spin state on the basis of the structural parameters of the analogous $[Fe^{III}(Him)_2(hapen)]^+$ [10–15].

At 100 K, four Fe–N bond distances are in the range 1.935(7)–2.005(6) Å, in which the Fe–N (imidazole) distance is slightly longer than the Fe–N (imine) distance. The Fe–O1 distance of 1.879(5) Å and the Fe–O2 distance of 1.879(6) Å are very close. These Fe–N and Fe–O coordination bond distances are consistent with the bond distances reported for LS $Fe^{III}$ complexes with similar Schiff-base ligands [10–15]. The averaged Fe–N bond distances decrease by 0.16 Å from 2.132 Å at 296 K to 1.968 Å at 100 K. The O1–Fe–O2 bond angle of 89.1(3)° is indicative of the LS spin state at 100 K on the basis of the structural parameters of the analogous $[Fe^{III}(Him)_2(hapen)]^+$, where HS compounds have a large angle around 104°, while SCO compounds have smaller angle around 101° [10–15]. The octahedral coordination geometry changes to a regular octahedron; especially, a large change is found in the O1–Fe–O2 bond angle, which decreases from 102.5(4)° at 296 K to 89.1(3)° at 100 K, a change of 13.4°. The five-membered chelate ring at 100 K assumes a gauche conformation, in which C9 and C10 atoms deviate by −0.20 and +0.41 Å from the plane defined by Fe, N1, and N2 atoms. The dihedral angle between the $N_2O_2$ coordination plane and the benzene moiety are −14.02° and 24.47° for benzene rings A and B, respectively, of which values are compared with −9.94° and 22.81° at 296 K. The molecular distortion of the complex-cation is quite tilted in the LS state, or, in other words, the LS state requires such a large distortion of $[Fe^{III}(Him)_2(hapen)]^+$.

As described above, and as shown in Table 2, noticeable structural deviations are found in the coordination bond distances and angles of Fe–N and O–Fe–O, and in the dihedral angle between the coordination plane and benzene rings. Figure 3 shows the minimized overlay of the complex-cation $[Fe^{III}(Him)_2(hapen)]^+$ in the HS state at 296 K and the LS state at 100 K, showing that large structural deviations are possible for the present complex-cation of $[Fe^{III}(Him)_2(hapen)]^+$ due to the steric repulsion between the methyl group of hapen and the five-membered chelate ring.

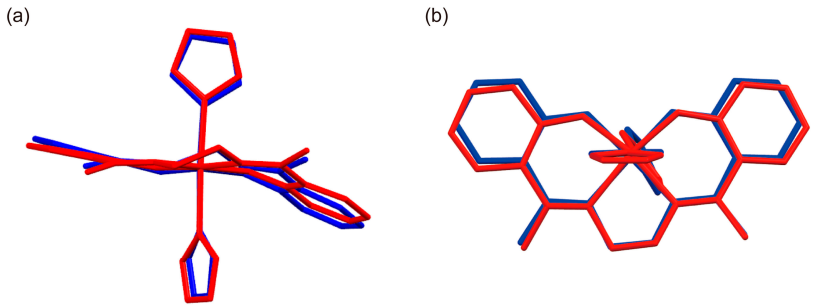


**Figure 3.** Minimized overlay of complex-cation λ-$[Fe^{III}(Him)_2(hapen)]^+$ in the HS state (red) at 296 K and the LS state (blue) at 100 K. (**a**) Top view; (**b**) Side view.

Figure 4a shows the one-dimensional (1D) zigzag-chain structure of $[Fe^{III}(Him)_2(hapen)]^+$ at 296 K, while the analogous compounds have various assembly structures, including the 1D structure [14–16]. The 1D structure running along the *b*-axis is constructed by inter-cation hydrogen bonding between a phenoxo oxygen O2 and an imidazole nitrogen N6* of the adjacent complex-cation, in which hydrogen

bond distance is O2···N6* = 2.95(1) Å. At 100 K, N6* of the imidazole group is bifurcated and hydrogen-bonded to O1 and O2, as shown in Figure 4b. As described above, there are difference between two Fe–O bond distances at 296 K, but not at 100 K. The adjacent complex-cations, linked by the hydrogen bonds, are related by a two-fold screw axis along the *b*-axis (* 1/2 − *x*, 1/2 + *y*, 1/2 − *z*), and the O2···N6* (O1···N6*) hydrogen bond is repeated to form a 1D structure running along the *b*-axis. As the complex-cation is a chiral species with δ-$[Fe^{III}(Him)_2(hapen)]^+$ or λ-$[Fe^{III}(Him)_2(hapen)]^+$ due to the δ-and λ-gauche conformation, the 1D chain is a chiral chain. The adjacent chains with opposite chiralities are arrayed alternately. The spin states are examined by the structural parameters. The unit cell volume decreases from 5596.5(7) $Å^3$ at 296 K to 5314.3(6) $Å^3$ at 100 K by 5.0% (1 − 5314.3/5596.7), where the reduction is as large as SCO $Fe^{II}$ complexes [1]. The cell dimensions of the three axes decrease; *a*-axis (−0.246 Å/*a*, 0.98%), *b*-axes (−0.376 Å/*b*, 3.8%), and *c*-axis (−0.432 Å/*c*, 1.7%). The data indicate that the change of the *b*-axis is the largest, which is in accordance with the 1D structure running along the *b*-axis.

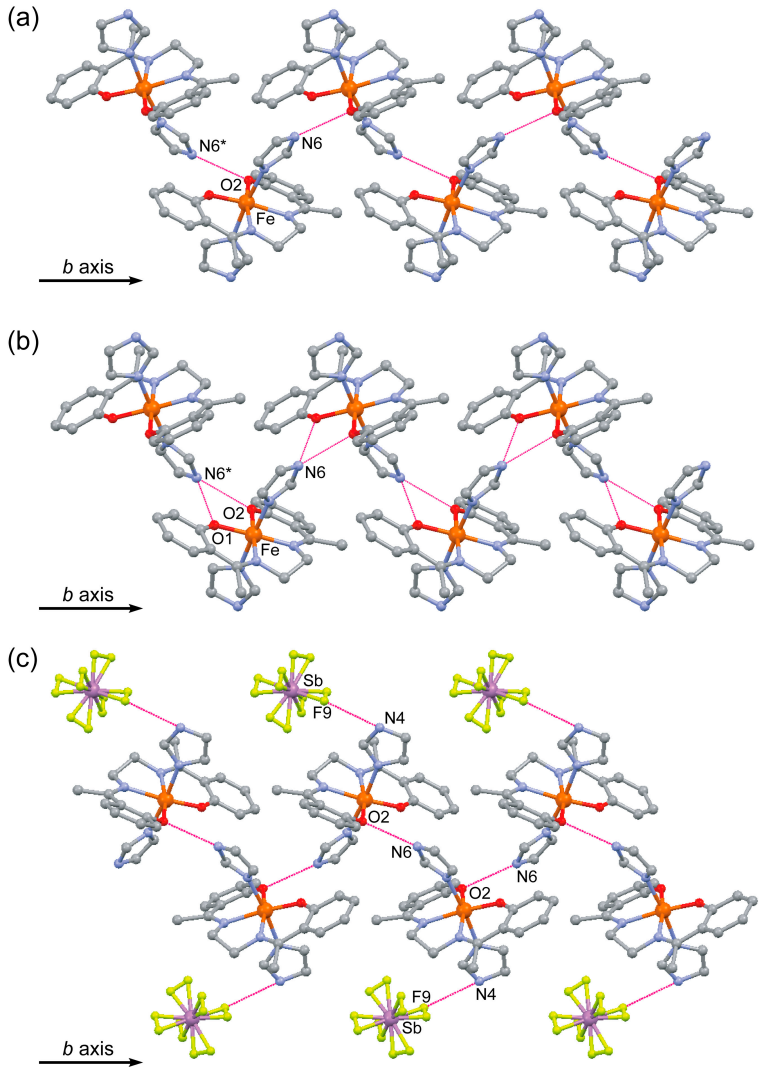


**Figure 4.** (**a**) 1D zigzag-chain structure constructed by the hydrogen bonds running along the *b*-axis, $\{\lambda\text{-}[Fe^{III}(Him)_2(hapen)]^+\}_{1\infty}$ at 296 K; (**b**) 1D zigzag-chain structure constructed by the inter-cation hydrogen along the *b*-axis at 100 K; (**c**) $SbF_6$ anions are weakly hydrogen-bonded to the 1D chain at 296 K.

As shown in Figure 4c, the remaining imidazole nitrogen atom N4 of the two imidazoles is close to the F3 and F9 atoms of the $SbF_6^-$ ion with N4···F3 = 3.10(3) and N4···F9 = 3.00(2) Å. On the other hand, the corresponding hydrogen bond distance is not found for the $PF_6$ and $AsF_6$ salts.

### *2.4. Spin Transition Profile and Temperature*

Three compounds of the $PF_6$, $AsF_6$, and $AsF_6$ salts of $[Fe^{III}(Him)_2(hapen)]Y$ have an isomorphous structure and show a one-step and abrupt SCO profile. (1) The complex-cation of $[Fe^{III}(Him)_2(hapen)]^+$ has a favorable molecular structure that can easily adapt the molecular distortion associated with the spin transition. During the spin transition from the HS to the LS state, the average Fe–N distance and O–Fe–O angle decrease by 0.16 Å and 13.4°, respectively, accompanying the molecular change of the coordination geometry from distorted octahedron to regular octahedron. (2) The abrupt SCO profile should be due to the hydrogen-bonded chiral one-dimensional assembly structure. Within a chiral chain, molecular expansion and contraction associated with the spin transition can be transmitted along the chain without resistance. (3) The spin transition temperature may be related to the cation-anion interaction and inter-chain interaction. The spin-transition temperature of the $PF_6$ salt is 78 K and that of the $AsF_6$ salt is $T_{1/2}\uparrow$ = 74.0 K and $T_{1/2}\downarrow$ = 69.4 K with 4.6 K thermal hysteresis. The spin-transition temperature of the present $SF_6$ salt is 105 K. The geometry of the anions, $PF_6$, $AsF_6$, and $AsF_6$, are the same and the difference is found in the anion size. The molecular volumes evaluated by the molecular mechanics calculation are $PF_6$ = 73.0 $Å^3$, $AsF_6$ = 78.5 $Å^3$, and $SbF_6$ = 88.7 $Å^3$ [17]. The order of the spin transition temperature is $AsF_6 < PF_6 < SbF_6$, while the order of the anion size is $PF_6 < AsF_6 < SbF_6$. There are many studies on the influence of the anion on the SCO properties for a series of SCO complexes [1,2,13]. The majority of the studies revealed that the larger the size of the anion, the lower the spin transition temperature. Our series of the complexes shows the reverse tendency; the larger the size of the anion, the higher the spin transition temperature. The remaining imidazole nitrogen atom N4 of the two imidazoles is close to the F3 and F9 atoms of the $SbF_6^-$ ion. On the other hand, the corresponding hydrogen bond is not found for the $PF_6$ and $AsF_6$ salts. The anion-cation interaction may be related to the spin transition temperature.

## 3. Experimental Section

All reagents and solvents used in this study are commercially available from Tokyo Kasei Co., Ltd., Tokyo, Japan, and Wako Pure Chemical Industries, Ltd., Osaka, Japan, and were used without further purification. All synthetic procedures were carried out in an open atmosphere.

### *3.1. Synthesis of $H_2$hapen and Precursor Iron(III) Complex $[Fe^{III}Cl(hapen)]\cdot 0.5CH_3OH$*

The tetradentate ligand $H_2$hapen and its precursor $Fe^{III}$ complex $[Fe^{III}Cl(hapen)]\cdot 0.5CH_3OH$ were prepared according to a previously reported method [14].

### *3.2. $[Fe^{III}(Him)_2(hapen)]SbF_6$*

An excess amount of imidazole (5.0 mmol, 0.34 g) was added to a suspension of $[Fe^{III}Cl(hapen)]\cdot 0.5CH_3OH$ (0.50 mmol, 0.20 g) in 15 mL of methanol, and the mixture was stirred for

15 min on a hot-plate and then filtered. A solution of $NaSbF_6$ (0.50 mmol, 0.13 g) in 5 mL of methanol was added to the filtrate and then filtered. The resulting solution was allowed to stand for a few days, during which time black plate-like crystals precipitated, and were collected by suction filtration and washed with a small amount of diethyl ether. Yield: 0.13 g (36%). Found: C, 39.94; H, 3.74; N, 11.60%. Calcd. for $[Fe^{III}(Him)_2(hapen)]SbF_6$ ($C_{24}H_{26}N_6O_2Fe{\cdot}SbF_6$): C, 39.92; H, 3.63; N, 11.64%.

### *3.3. Physical Measurements*

Elemental analyses (C, H, and N) were carried out at the Center for Instrumental Analysis of Kumamoto University. Magnetic susceptibilities were measured by a Quantum Design (San Diego, CA, USA) MPMS-XL5 magnetometer in the temperature range of 5–300 K at a scan rate of 0.5 K $min^{-1}$ under an applied magnetic field of 0.5 T. The magnetic susceptibilities were measured while lowering the temperature from 300 to 5 K in the first run. In the second run, the magnetic susceptibility was measured while raising the temperature from 5 to 300 K. The calibration was performed with palladium metal. Corrections for diamagnetism were applied using Pascal's constants.

### *3.4. X-Ray Crystallography*

X-ray diffraction data were collected using a Rigaku (Tokyo, Japan) RAXIS RAPID imaging plate diffractometer using graphite monochromated Mo Kα radiation (λ = 0.71073 Å). The temperature of the crystal was maintained at the selected temperature by means of a Rigaku cooling apparatus. The X-ray diffraction data for $[Fe^{III}(Him)_2(hapen)]SbF_6$ were collected at 296 and 100 K. The data were corrected for Lorentz, polarization, and absorption effects. The structures were solved using a direct method, and expanded using the Fourier technique. Hydrogen atoms were fixed at the calculated positions and refined using a riding model. All calculations were performed using the CrystalStructure crystallographic software package (CrystalStructure 4.0, Tokyo, Japan). The X-ray crystallographic data in a CIF format have been deposited with CCDC (reference numbers CCDC 926685 and 926686). They can be obtained free of charge at http://www.ccdc.cam.ac.uk /conts/retrieving.html, or from the Cambridge Crystallographic Data Centre, 12 Union Road, Cambridge CB2 1EZ, UK; fax: (+44) 1223-336-033; or e-mail: deposit@ccdc.cam.ac.uk.

## 4. Conclusions

A family of the SCO $Fe^{III}$ complexes $[Fe^{III}(Him)_2(hapen)]Y$ shows a one-step and abrupt SCO profile. The present work can reveal how the series of the compounds can exhibit such a SCO property. The complex-cation of $[Fe^{III}(Him)_2(hapen)]^+$ has a favorable molecular structure that can easily adapt the molecular distortion between a distorted and regular octahedron, especially found in the large change of O–Fe–O angle. The abrupt SCO profile should be due to the intermolecular imidazole…phenoxo hydrogen-bonded chiral one-dimensional assembly structure. Within a chiral chain, molecular expansion and contraction associated with the spin transition can be transmitted along the chain. The spin transition temperature may be related to the cation-anion interaction and inter-chain interaction. The spin-transition temperature of the $PF_6$ salt is 78 K and that of the $AsF_6$ salt is $T_{1/2}\uparrow$ = 74.0 K and $T_{1/2}\downarrow$ = 69.4 K with 4.6 K thermal hysteresis. The spin-transition temperature of the present $SF_6$ salt is 105 K. The order of the spin

transition temperature is $AsF_6 < PF_6 < SbF_6$, while the order of the anion size is $PF_6 < AsF_6 < SbF_6$. The anion-cation interaction may be related to the spin transition temperature.

## Author Contributions

The experimental work was performed mainly by T.U. and assisted by K.M., D.H., H.O. and T.F.. Y.S. performed the magnetic measurements. T.F. supported the work and supervised the experimental work. The manuscript was written by N.M. and T.U. All authors have given approval for the final version of the manuscript.

## Conflicts of Interest

The authors declare no conflict of interest.

## References and Notes

1. Gütlich, P.; Goodwin, H.A. *"Spin Crossover in Transition Metal Compounds I–III": Topics in Current Chemistry*; Springer: New York, NY, USA, 2004.
2. Weber, B.; Bauer, W.; Obel, J. An Iron (II) Spin-Crossover Complex with a 70 K Wide Thermal Hysteresis Loop. *Angew. Chem. Int. Ed.* **2008**, *47*, 10098–10101.
3. Yamada, M.; Hagiwara, H.; Torigoe, H.; Matsumoto, N.; Kojima, K.; Dahan, F.; Tuchagues, J.P.; Re, N.; Iijima. S. A Variety of Spin-Crossover Behaviors Depending on the Counter Anion: Two-Dimensional Complexes Constructed by NH Cl⁻ Hydrogen Bonds, $[Fe^{II}H_3L^{Me}]Cl\cdot X$ ($X = PF_6^-$, $AsF_6^-$, $SbF_6^-$, $CF_3SO_3^-$; $H_3L^{Me}$ = Tris[2-{[(2-methylimidazol-4-yl)methylidene]-amino}ethyl]amine). *Chem. Eur. J.* **2006**, *12*, 4536–4549.
4. Sato, T.; Nishi, K.; Iijima, S.; Kojima , M.; Matsumoto, N. One-Step and Two-Step Spin-Crossover Iron(II) Complexes of ((2-Methylimidazol-4-yl)methylidene)histamine. *Inorg. Chem.* **2009**, *48*, 7211–7229.
5. Nishida, Y.; Oshio, S.; Kida, S. Investigation on crossover complexes. Magnetic properties of iron(III) complexes with several Schiff bases. *Chem. Lett.* **1975**, 79–80.
6. Nishida, Y.; Oshio, S.; Kida, S. Synthesis and magnetic properties of iron (III) complexes with several quadridentate Schiff bases. *Bul. Chem. Soc. Jpn.* **1977**, *50*, 119–122.
7. Matsumoto, N.; Kimoto, K.; Nishida, K.; Ohyoshi, A. Spin-State Equilibrium of Iron(III) Complex with Planar Unsymmertical Quadridentate Schiff Base in Solution. *Chem. Lett.* **1984**, 479–480.
8. Matsumoto, N.; Kimoto, K.; Ohyoshi, A.; Maeda, Y.; Okawa, H. Synthesis and characterization of iron(III) complexes with unsymmetrical quadridentate Schiff bases, and spin equilibrium behavior in solution. *Bull. Chem. Soc. Jpn.* **1984**, *57*, 3307–3311.
9. Maeda, Y.; Takashima, Y.; Matsumoto, N.; Ohyoshi, A. Spectroscopic and Magnetic Properties of $[FeL_2(salacen)]PF_6$ (L = Imidazole or N-Methylimidazole): New Examples of Intermediate Electronic Relaxation between *S*=1/2 and *S*=5/2 States. X-Ray Crystal Structure of $[Fe(Him)_2(salacen)]PF_6$. *J. Chem. Soc. Dalton Trans*. **1986**, 1115–1123.

10. Kennedy, B.J.; McGrath, A.C.; Murray, K.S.; Skelton, B.W.; White A.H. Variable-temperature magnetic, spectral, and x-ray crystallographic studies of "spin-crossover" iron(III) Schiff-base-Lewis-base adducts. Influence of non-coordinated anions on spin-state interconversion dynamics in [Fe(salen)(imd)$_2$]Y species (Y = $ClO_4^-$, $BF_4^-$, $PF_6^-$, $BPh_4^-$; imd = imidazole). *Inorg. Chem.* **1987**, *26*, 483–495.
11. Ross, T.M.; Neville, S.M.; Innes, D.S.; Turner, D.R.; Moubaraki, B.; Murray, K.S. Spin crossover in iron(III) Schiff-base 1-D chain complexes. *Dalton Trans.* **2010**, *39*, 149–159.
12. Hernandenz-Molia R.; Mederis, A.; Dominguez, S.; Gili, P.; Ruiz-Perez, C.; Castineiras, A.; Solans, X.; Lloret, F.; Real, J.A. Different ground spin states in iron (III) complexes with quadridentate Schiff bases: Synthesis, crystal structures, and magnetic properties. *Inorg. Chem.* **1998**, *37*, 5102–5108.
13. Halcrow, M.A. Structure:function relationships in molecular spin-crossover complexes. *Chem. Soc. Rev.* **2011**, *40*, 4119–4142.
14. Koike, M.; Murakami, K.; Fujinami, T.; Nishi, K.; Matsumoto, N.; Sunatsuki, Y. Syntheses, three types of hydrogen-bonded assembly structures, and magnetic properties of [$Fe^{III}$(Him)$_2$(hapen)]Y·solvent (Him = imidazole, hapen = *N,N′*-bis(2-hydroxyacetophenylidene)ethylenediamine, Y = $BPh_4^-$, $CF_3SO_3^-$, $PF_6^-$, $ClO_4^-$, and $BF_4^-$). *Inorg. Chim. Acta* **2013**, *399*, 185–192.
15. Fujinami, T.; Koike, M.; Matsumoto, N.; Sunatsuki, Y.; Okazawa, A.; Kojima, N. Abrupt spin transition with thermal hysteresis of iron(III) complex [$Fe^{III}$(Him)$_2$(hapen)]$AsF_6$ (Him = imidazole, $H_2$hapen = *N,N′*-bis(2-hydroxyacetophenylidene)ethylenediamine). *Inorg. Chem.* **2014**, *53*, 2254–2259.
16. Fujinami, T.; Ikeda, M.; Koike, M.; Matsumoto, N.; Oishi, T.; Sunatsuki, Y. Syntheses, hydrogen-bonded assembly structures, and spin crossover properties of [$Fe^{III}$(Him)$_2$(*n*-MeOhapen)]$PF_6$ (Him = imidazole and *n*-MeOhapen = *N,N′*-bis(*n*-methoxy-2-oxyacetophenylidene)ethylenediamine); *n* = 4, 5, 6). *Inorg. Chim. Acta* **2015**, *432*, 89–95.
17. *Spartan*, Version 10; Wavefunction Inc.: Irvine, CA, USA, 2011.